Ground-State Electronic Structure of the Dimer-of-Dimers Complex $[(Mn_2O_2)_2(tphpn)_2]^{4+}$: Potential Relevance to the Photosystem II Water Oxidation Catalyst

Martin L. Kirk,[†] Michael K. Chan,[‡] William H. Armstrong,*[,‡,§] and Edward I. Solomon*[,†]

Contribution from the Department of Chemistry, Stanford University, Stanford, California 94304, and the Department of Chemistry, University of California, Berkeley, California 94720.
Received June 3, 1992

Abstract: The tetrameric dimer-of-dimers complex $[(Mn_2O_2)_2(tphpn)_2]^{4+}$ possesses structural features and a parallel polarization EPR spectrum which are similar to those observed for the S_1 state of the photosystem II water oxidation catalyst. We have probed the ground-state electronic structure of $[(Mn_2O_2)_2(tphpn)_2]^{4+}$ by magnetic susceptibility and isothermal saturation magnetization measurements to understand the origin of the EPR spectrum in terms of the intra- and interdimer magnetic exchange interactions and the ground-state zero-field splitting. Both $[Mn^{III}Mn^{IV}]$ dimers are treated as having an effective spin $S' = {}^1/_2$ which are coupled ($J' = +38.8$ cm^{-1}) to yield a zero-field split ($D = +1.8$ cm^{-1}, $E = -0.15$ cm^{-1}) triplet ground state. The fictitious J' has been related by vector algebra methods to the real J that describes the exchange through the alkoxide oxygen atoms of the tphpn ligands ($J' = -4J_{alkoxide}$). This treatment shows that the effective ferromagnetic interaction between the two $S' = {}^1/_2$ cores has its origin in an alkoxide mediated antiferromagnetic exchange interaction. The difference in the magnitude of the singlet-triplet splitting obtained via the effective model and that obtained using a model describing the full exchange symmetry of the tetramer is on the order of 1%. It has been determined that the zero-field splitting is not of single ion or dipolar origin but results from pseudodipolar coupling. We have shown that the electronic structure of $[(Mn_2O_2)_2(tphpn)_2]^{4+}$ parallels the geometric structure of the complex, and these results are presented in light of their relevance to the manganese water oxidation catalyst.

Introduction

The active site for water oxidation in photosystem II (PSII) consists of a polynuclear manganese aggregate that has been studied extensively with physical techniques such as magnetic susceptibility, electron paramagnetic resonance (EPR), X-ray absorption (XAS), and electron spin echo envelope modulation (ESEEM) spectroscopies. The water oxidation catalyst (WOC) undergoes four sequential one-electron oxidations before the liberation of molecular oxygen and regeneration of the catalyst.[1] These five oxidation levels are known as the Kok S states[2] and are labeled S_0-S_4. Although the actual structure of the water oxidation catalyst is not yet defined, spectral data place limitations on structures that may be proposed for some of the S states. Specifically, the extended fine structure region of the XAS spectrum clearly indicates that there are at least two ~2.7 Å Mn···Mn interactions for the S_2 state.[3-5] A longer Mn···Mn interaction at ~3.3 Å has also been proposed from the EXAFS data,[4,5] although this may result from a Mn···Ca interaction. XAS studies in the edge and pre-edge region support an oxidation state assignment of Mn(III,IV,IV,IV) for the manganese aggregate at the S_2 level.[5b] The principle EPR signals associated with the manganese site in functional PSII include, for the Kok S_2 state, a "multiline" signal (at least 19 hyperfine components) centered at $g = 2$ and a second lower field signal at $g = 4.1$.[3] Fine structure on the $g = 4.1$ signal, recently detected by Kim et al.,[6] indicates that it is also associated with a polynuclear center. The $g = 2$ and $g = 4.1$ EPR signals can be interconverted and have been interpreted in terms of an odd-electron configuration. When the manganese aggregate is at the S_1 level, an even-electron configuration should then be present. X-ray edge studies at S_1 are consistent with a Mn(III,IV,III,IV) oxidation state although a Mn(III,III,III,III) oxidation state cannot be ruled out.[5b,c] The EXAFS data show no discernible structural change occurs between S_1 and S_2.[5b,c] Dexheimer and Klein have recently detected a parallel polarization mode EPR signal associated with the manganese active site at the S_1 oxidation level.[7] The broad derivative signal, which is centered at $g = 4.8$, has been simulated using a rhombic $S = 1$ spin-Hamiltonian with $g = 2$, and zero-field splitting (ZFS) parameters of $D = 0.125$ cm^{-1} and $E = 0.025$ cm^{-1}.

The approach we and others[8] are taking to further elucidate the structure of the PSII polynuclear manganese water oxidation catalyst (MnWOC) involves the synthesis and characterization of plausible small molecule analogs. In recent years these synthetic efforts have provided a wide variety of polynuclear manganese oxo aggregates of potential relevance to the biological system. Compounds containing from two to twelve manganese atoms have

[†] Stanford University.
[‡] University of California.
[§] Current address: Department of Chemistry, Boston College, Chestnut Hill, MA 02167.

(1) (a) Joliet, P.; Barbieri, G.; Chabaud, R. *Photochem. Photobiol.* **1970**, *10*, 309-329. (b) Joliet, P.; Joliet, A.; Bouges, B.; Barbieri, G. *Photochem. Photobiol.* **1971**, *14*, 287-305.

(2) Kok, B.; Forbush, B..; McGloin, M. *Photochem. Photobiol.* **1970**, *11*, 457-475.

(3) (a) Renger, G. *Angew. Chem., Int. Ed. Engl.* **1989**, *26*, 643-660. (b) Babcock, G. T. In *New Comprehensive Biochemistry: Photosynthesis*: Amesz, J., Ed.; Elsevier: Amsterdam, 1987; pp 125-158. (c) Govindjee; Kambara, T.; Coleman, W. *Photochem. Photobiol.* **1985**, *42*, 187-210. (d) Dismukes, G. *Photochem. Photobiol.* **1986**, *43*, 99-115. (e) Brudvig, G. W. In *Metal Clusters in Proteins*; Que, L., Jr., Ed.; ACS Symposium Series 372; American Chemical Society: Washington, DC, 1988; pp 221-237. (f) Babcock, G. T.; Barry, B. A.; Debus, R. J.; Hoganson, C. W.; Atamian, M.; McIntosh, L.; Sithole, I.; Yocum, C. F. *Biochemistry* **1989**, *28*, 9557-9565.

(4) (a) George, G. N.; Prince, R. C.; Cramer, S. P. *Science* **1989**, *243*, 789-791. (b) Kirby, J. A.; Robertson, A. S.; Smith, J. P.; Thompson, A. C.; Cooper, S. R.; Klein, M. P. *J. Am. Chem. Soc.* **1981**, *103*, 5529-5537. (c) McDermott, A. E.; Yachandra, V. K.; Guiles, R. D.; Cole, J. L.; Dexheimer, S. L.; Britt, R. D.; Sauer, K.; Klein, M. P. *Biochemistry* **1988**, *27*, 4021-4031.

(5) (a) Guiles, R. D.; Zimmermann, J.-L.; McDermott, A. E.; Yachandra, V. K.; Cole, J. L.; Dexheimer, S. L.; Britt, R. D.; Weighardt, K.; Bossek, U.; Sauer, K.; Klein, M. P. *Biochemistry* **1990**, *29*, 471-485. (b) Guiles, R. D.; Yachandra, V. K.; McDermott, A. E.; DeRose, V. J.; Zimmermann, J.-L.; Sauer, K.; Klein, M. P. In *Current Research in Photosynthesis*; Battscheffsky, M., Ed.; Kluwer Academic Publishers: Netherlands, 1990; Vol. I, pp 789-792. (c) Sauer, K.; Yachandra, V. K.; Britt, R. D.; Klein, M. P. In *Manganese Redox Enzymes*; Pecoraro, V. L., Ed.; VCH Publishers: New York, 1992; pp 141-175.

(6) Kim, D. H.; Britt, R. D.; Klein, M. P.; Sauer, K. *Biochemistry* **1992**, *31*, 541-547.

(7) (a) Dexheimer, S. L.; Klein, M. P.; Sauer, K. In *Current Research in Photosynthesis*; Battscheffsky, M., Ed.; Kluwer Academic Publishers: Netherlands, 1990; Vol. I, pp 761-764. (b) Dexheimer, S. L.; Klein, M. P. *J. Am. Chem. Soc.* **1992**, *114*, 2821-2826.

(8) (a) Pecoraro, V. L. *Photochem. Photobiol.* **1988**, *48*, 249-246. (b) Christou, G. *Acc. Chem. Res.* **1989**, *22*, 328-335. (c) Weighardt, K. *Angew. Chem., Int. Ed. Engl.* **1989**, *28*, 1153-1172. (d) Brudvig, G. W.; Crabtree, R. H. *Prog. Inorg. Chem.* **1989**, *37*, 99-142.

0002-7863/92/1514-10432$03.00/0

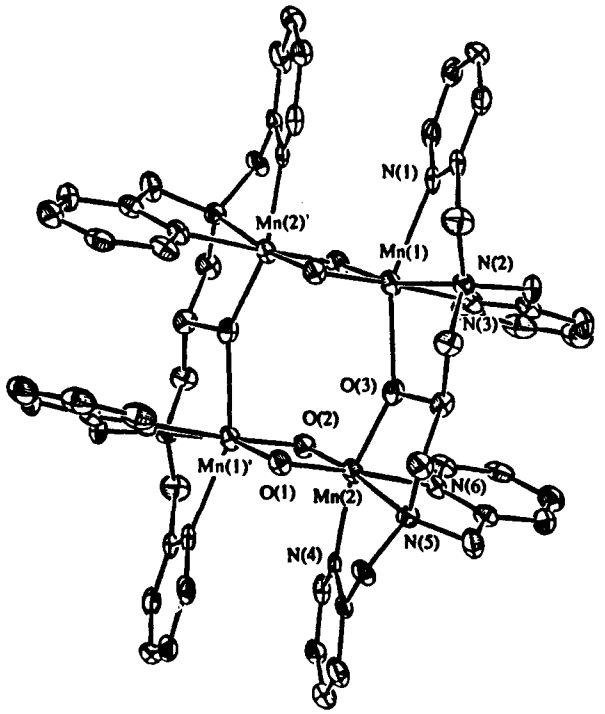

Figure 1. Structure of the dimer-of-dimers complex $[(Mn_2O_2)_2(tphpn)_2]^{4+}$ with thermal ellipsoids at 50% probability. Hydrogen atoms have been omitted for clarity. Primed and unprimed atoms are related by inversion symmetry.

been isolated.[8b] Complexes containing the $\{Mn_2(\mu\text{-}O)_2\}^{n+}$ core, many of which have been reported,[9] have Mn···Mn distances of approximately 2.7 Å and as such this core can be thought of as a substructure of the MnWOC. In the $n = 3$ core oxidation state (i.e., $Mn^{III}Mn^{IV}$) these binuclear cores are strongly antiferromagnetically exchange coupled ($J = -118$ to -159 cm^{-1}; $\mathcal{H} = -2JS_1 \cdot S_2$ for $S_{1(Mn(III))} = 2$ and $S_{2(Mn(IV))} = {}^3/_2$) producing a $S_{tot} = {}^1/_2$ ground state which typically displays $g = 2$ X-band EPR signals with 16 principal hyperfine components.[9] Qualitatively, the multiline EPR signature for $\{Mn_2O_2\}^{3+}$ species is similar to that of the MnWOC at the S_2 oxidation level; however, the latter usually has several more lines and is markedly broader. Thus, $\{Mn_2O_2\}$ binuclear species can be thought of as first generation models for the MnWOC. However, based on the EPR spectral data it is unlikely that the biological aggregate is composed of isolated $\{Mn_2O_2\}$ subunits.

One configuration of manganese ions that is consistent with the EXAFS results at the S_1 and S_2 oxidation levels is a dimer-of-dimers[10] structure consisting of two tethered $\{Mn_2O_2\}$ cores.[5] It was conjectured that the heptadentate ligand tphpn (*N*,*N*,*N*′,*N*′-tetra(2-methylpyridyl)-2-hydroxypropanediamine) is well set up to promote the formation of such a target structure. After characterizing two structurally distinct tetranuclear species,[11] we isolated a complex with the $\{Mn_2O_2\}_2^{6+}$ core, as reported recently.[12] The structure of $[(Mn_2O_2)_2(tphpn)_2]^{4+}$ is shown in Figure 1 and consists of two $\{Mn_2O_2\}^{3+}$ core units bridged by the alkoxide oxygens of the tphpn ligand such that a Mn(III) is linked to a Mn(IV) of an opposite dimer.[13] This complex displays a parallel polarization EPR signal that closely resembles that associated with the S_1 state of the MnWOC in PSII.[7,12] In this study, we evaluate this model in the context of what is known about the MnWOC, describe the origin of the parallel polarization EPR resonance, and, in general, develop an overall electronic structure description of $[(Mn_2O_2)_2(tphpn)_2]^{4+}$.

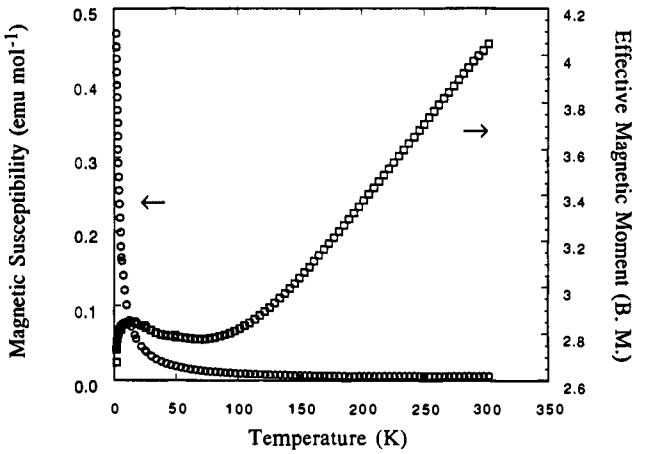

Figure 2. Magnetic susceptibility (circles) and effective magnetic moment (squares) of $[(Mn_2O_2)_2(tphpn)_2]^{4+}$. The applied magnetic field is 3000 G.

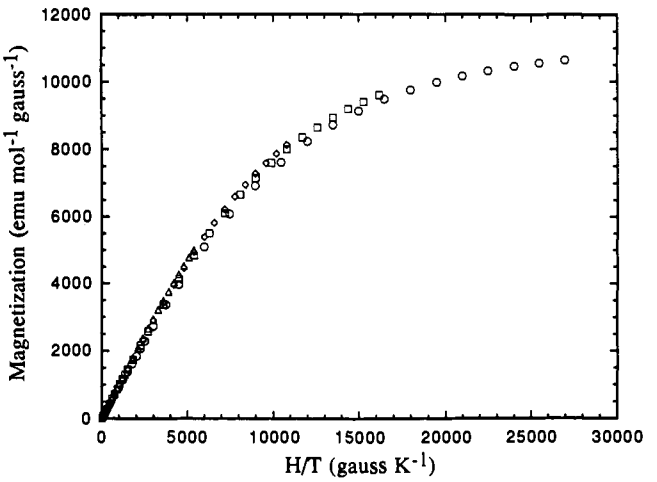

Figure 3. Isothermal magnetization as a function of H/T. Data collected at 2.0 K (circles), 3.33 K (squares), 5.0 K (diamonds), and 10.0 K (triangles) in applied magnetic fields up to 54 kG.

(9) (a) Hagen, K. S.; Armstrong, W. H.; Hope, H. *Inorg. Chem.* **1988**, *27*, 967–969. (b) Plaskin, P. M.; Stoufer, R. C.; Mathew, M.; Palenik, G. J. *J. Am. Chem. Soc.* **1972**, *94*, 2121–2122. (c) Stebler, M.; Ludi, A.; Bürgi, H.-B. *Inorg. Chem.* **1986**, *25*, 4743–4750. (d) Collins, M. A.; Hodgson, D. J.; Michelsen, K.; Towle, D. K. *J. Chem. Soc., Chem. Commun.* **1987**, 1659–1660. (e) Towle, D. K.; Botsford, C. A.; Hodgson, D. J. *Inorg. Chim. Acta* **1988**, *141*, 167–168. (f) Suzuki, M.; Tokura, S.; Suhara, M.; Uehara, A. *Chem. Lett.* **1988**, 477–480. (g) Hoof, D. L.; Tisley, K. G.; Walton, R. A. *Inorg. Nucl. Chem. Lett.* **1973**, *9*, 571–576. (h) Goodson, P. A.; Hodgson, D. J. *Inorg. Chem.* **1989**, *28*, 3606–3608. (i) Libby, E.; Webb, R. J.; Streib, W. E.; Folting, K.; Huffman, J. C.; Hendrickson, D. N.; Christou, G. *Inorg. Chem.* **1989**, *28*, 4037–4040. (j) Brewer, K. J.; Liegeois, A.; Otvos, J. W.; Calvin, M.; Spreer, L. O. *J. Chem. Soc., Chem. Commun.* **1988**, 1219–1220. (k) Suzuki, M.; Senda, H.; Kobayashi, Y.; Oshio, H.; Uehara, A. *Chem. Lett.* **1988**, 1763–1766. (l) Goodson, P. A.; Glerup, J.; Hodgson, D. J.; Michelsen, K.; Pedersen, E. *Inorg. Chem.* **1990**, *29*, 503–508. (m) Cooper, S.; Calvin, M. *J. Am. Chem. Soc.* **1977**, *99*, 6623–6630. (n) Brewer, K. J.; Calvin, M.; Lumpkin, R. S.; Otvos, J. W.; Spreer, L. O. *Inorg. Chem.* **1989**, *28*, 4446–4451. Goodson, P. A.; Hodgson, D. J.; Michelsen, K. *Inorg. Chim. Acta* **1990**, *172*, 49–52.

(10) The term dimer-of-dimers is used throughout the manuscript to refer to two dimers, each strongly exchange coupled, with a weak exchange coupling between them.

(11) (a) Chan, M. K.; Armstrong, W. H. *J. Am. Chem. Soc.* **1989**, *111*, 9121–9122. (b) Chan, M. K.; Armstrong, W. H. *J. Am. Chem. Soc.* **1990**, *112*, 4985–4986.

(12) (a) Chan, M. K.; Armstrong, W. H. *J. Am. Chem. Soc.* **1991**, *113*, 5055–5057. (b) Chan, M. K. Ph.D. Dissertation, University of California, Berkeley, CA, 1991.

(13) The $[(Mn_2O_2)_2(tphpn)_2]^{4+}$ cation resides on a crystallographic inversion center (monoclinic space group $P2_1/c$). The two $\{Mn_2(\mu\text{-}O)_2\}$ core units possess bond distances and angles which are nearly identical to those found in the structurally characterized di-μ-oxo dimer complexes (see ref 9). The crystal structure shows an elongation along the $Mn^{III}(1)$–N(1) and $Mn^{III}(1)$–$O(3)_{alkoxide}$ bonds with respect to the *in*-plane bond distances. As a result of this structural distortion and the dominant ligand field created by the in-plane oxo ligands, the ground state of the Mn(III) ion in this complex should be $d_{x^2-y^2}$ (hole formalism) with the d_{z^2} orbital singly occupied. This situation is the same as that found for Mn(III) in the isolated di-μ-oxo dimer compounds.

Experimental Section

Preparation of the heptadentate ligand tphpn and $[(Mn_2O_2)_2(tphpn)_2(H_2O)(CF_3SO_3)_2]^{3+}$ have been described elsewhere.[11] The title complex $[(Mn_2O_2)_2(tphpn)_2](ClO_4)_4 \cdot 3H_2O \cdot 2CH_3COCH_3$ was prepared as previously described[12] by vapor diffusion of acetone into an acetonitrile solution of $[Mn_4O_2(tphpn)_2(H_2O)_2(CF_3SO_3)_2]^{3+}$ followed by recrystallization from MeCN/acetone.

Magnetic susceptibility data were collected in the temperature range 2.0–300 K and in applied magnetic fields up to 54 kGauss with the use of a Quantum Design Model MPMS SQUID magnetometer. Mercury tetrathiocyanatocobaltate(II) and a palladium cylinder were employed as duel magnetometer calibrants. Pascal's constants were used to determine the constituent atom diamagnetism.[14] A 17.01-mg sample of powdered $[(Mn_2O_2)_2(tphpn)_2](ClO_4)_4$ was contained in the small half of a gelatin capsule and capped with a cotton plug. A phenolic guide (clear soda straw) was used to house the sample holder and was fixed to the end of the magnetometer drive rod. The measured diamagnetism of the entire sample holder assembly was approximately 25% of the measured magnetization at 300 K and 3 kOe. Standard library routines for matrix diagonalization and function minimization were used in the analysis of the data.

Results

The temperature dependence of the magnetic susceptibility and the effective magnetic moment are shown in Figure 2. The magnetic moment differs considerably from that observed in Mn(III)/Mn(IV) di-μ-oxo complexes, and its temperature dependence can be considered in three regions. At 15 K, there is a maximum in μ_{eff} which rapidly drops off with decreasing temperature, being characteristic of a zero-field split spin system. Between 15 and 150 K the behavior is quite complex. The moment decreases with increasing temperature from 15 K, goes through a broad minimum at ~75 K, and then increases with temperature. The initial decrease is suggestive of populating a state or states with lower spin multiplicity than that of the ground state. Above 150 K the moment increases in a manner reminiscent of Mn(III)–Mn(IV) di-μ-oxo dimer complexes. Isothermal magnetization data are plotted as a function of H/T in Figure 3. Complete saturation is not achieved, even at the highest applied field and the lowest temperature. This could be due to the presence of more than one Zeeman component contributing to the Boltzmann population or to the effects of temperature independent paramagnetism. The latter phenomenon results from magnetic field induced mixing of excited-state wave functions into the ground state. The data acquired at different temperatures are superimposable, showing no evidence for nesting. This behavior is characteristic of the presence of small substate splittings and negligible field induced mixing between thermally populated spin states.

Analysis

Effective Exchange Formalism. The dimer cores of $[(Mn_2O_2)_2(tphpn)_2](ClO_4)_4$ are essentially structurally identical to those found in isolated Mn(III)/Mn(IV) di-μ-oxo dimer complexes.[9,13] All known Mn(III/IV) di-μ-oxo dimer complexes are strongly antiferromagnetically exchange coupled with doublet–quartet splittings ($3J_1$) of approximately 360–480 cm^{-1}.[9] Reduced coupling has been observed in the Mn(III)–Mn(IV) alkoxide-bridged dimer complex $[Mn^{III}Mn^{IV}[2\text{-}OH\text{-}3,5\text{-}Cl_2\text{-}(SALPN)]_2(THF)]ClO_4$,[15] which possesses a 3.65 Å Mn–Mn distance and a J value of -10 cm^{-1}. Therefore, the interdimer interaction (J_2) in $[(Mn_2O_2)_2(tphpn)_2](ClO_4)_4$ should be at least an order of magnitude smaller than that within the di-μ-oxo cores (J_1) since the former derives from a long (3.96 Å) Mn–alkoxide–Mn bridge. Due to the large exchange coupling observed in di-μ-oxo bridged dimers, only the $S = {}^1/_2$ state is populated at low temperatures. In this limit, the dimer-of-dimers complex $[(Mn_2O_2)_2(tphpn)_2](ClO_4)_4$ may *effectively* be treated as a weakly interacting $S_a = S_b = {}^1/_2$ spin system with a singlet–triplet splitting of $2J'$. This situation is depicted schematically in Figure 4. We note that in the following section this model is evaluated by solving the complete exchange problem involving both the intradimer (J_1) and interdimer (J_2) exchange interactions.

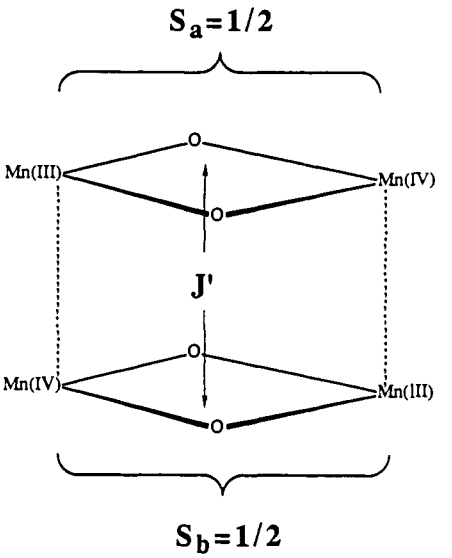

Figure 4. Schematic representation of the dimer-of-dimers effective exchange formalism. If the interdimer interaction (J_2) is assumed to be at least an order of magnitude smaller than the Mn(III,IV) di-μ-oxo intradimer interaction (J_1), the system may *effectively* be treated as a weakly interacting $S_a = S_b = {}^1/_2$ spin system with a singlet–triplet splitting of $2J'$.

We use primes to denote spin-Hamiltonian parameters within the effective scheme. Two equivalent approaches may be taken at this point. One may perform operations on the coupled $\langle S,m|$ basis or the uncoupled $\langle S_a\ m_{sa}, S_b\ m_{sb}|$ basis. Although the two are related by Clebsch–Gordon coefficients such that

$$\langle 1,1| = \langle {}^1/_2\ {}^1/_2, {}^1/_2\ {}^1/_2|$$

$$\langle 1,0| = \sqrt{2}\langle {}^1/_2\ {}^1/_2, {}^1/_2\ -{}^1/_2| + \sqrt{2}\langle {}^1/_2\ -{}^1/_2, {}^1/_2\ {}^1/_2|$$

$$\langle 1,-1| = \langle {}^1/_2\ -{}^1/_2, {}^1/_2\ -{}^1/_2|$$

$$\langle 0,0| = \sqrt{2}\langle {}^1/_2\ {}^1/_2, {}^1/_2\ -{}^1/_2| - \sqrt{2}\langle {}^1/_2\ -{}^1/_2, {}^1/_2\ {}^1/_2|$$

it is convenient to work within the uncoupled basis when orientational averaging is considered and the strong exchange limit ($J \gg D \sim g\beta H$) cannot be assumed a priori (i.e., the total spin is not a good quantum number). The spin-Hamiltonian (1)

$$\mathcal{H} = 2J'_x(S_{ax}\cdot S_{bx}) - 2J'_y(S_{ay}\cdot S_{by}) - 2J'_z(S_{az}\cdot S_{bz}) + g'_x\beta H\cdot(S_{ax} + S_{bx}) + g'_y\beta H\cdot(S_{ay} + S_{by}) + g'_z\beta H\cdot(S_{az} + S_{bz}) \quad (1)$$

was used to operate on the uncoupled basis functions. An anisotropic exchange Hamiltonian[16] was used in order to account for any zero-field splitting (ZFS) of the triplet state. In order to avoid problems associated with overparameterization during function minimization, the g tensor has been assumed to be isotropic ($g'_x = g'_y = g'_z$). Diagonalization of the resultant matrix yielded four energy eigenvalues which were substituted into the thermodynamic expression for the magnetic susceptibility (2)

$$\chi_{\cos\theta} = -\frac{N}{H}\left[\frac{\sum_i \frac{\delta E_i}{\delta H}\exp\left(\frac{-E_i}{kT}\right)}{\sum_i \exp\left(\frac{-E_i}{kT}\right)}\right] \quad (2)$$

(14) (a) Figgis, B. N.; Lewis, J. In *Modern Coordination Chemistry*; Lewis, J.; Wilkins, R. G. Eds.; Interscience: New York, 1960; Chapter 6, p 403. (b) Konig, E. *Magnetic Properties of Transition Metal Compounds*; Springer-Verlag: West Berlin, 1966. (c) Weller, R. R.; Hatfield, W. E. *J. Chem. Ed.* **1979**, *56*, 652.

(15) Larson, E.; Haddy, A.; Kirk, M. L.; Sands, R. H.; Hatfield, W. E.; Pecoraro, V. L. *J. Am. Chem. Soc.* **1992**, *114*, 6263–6265.

(16) Abragam, A.; Bleaney, B. In *Electron Paramagnetic Resonance of Transition Ions*; Dover Publications, Inc.: New York, 1986; pp 521–535.

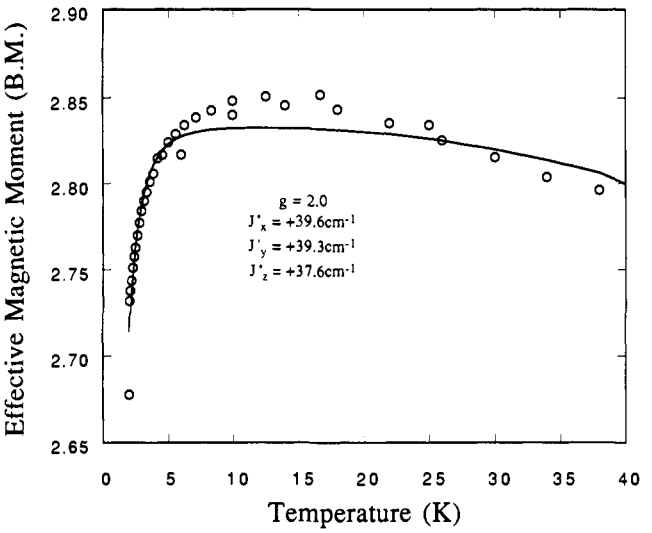

Figure 5. Fit of the effective magnetic moment in the temperature range 2–40 K using the effective formalism. The curve through the data is derived from the best-fit parameters.

where $\chi_{\cos\theta}$ is the molar magnetic susceptibility with the magnetic field direction at an angle θ with respect to the principle axis of the molecule. The partial derivatives with respect to the applied magnetic field, $\partial E/\partial H$, were calculated using the Hellman–Feynman theorem.[17] This method utilizes the eigenvectors obtained directly from the matrix diagonalization to determine $\partial E/\partial H$ exactly. Numerical methods for determining this partial derivative are approximate and require function evaluation at two additional magnetic fields about the actual applied field. A numerical integration technique utilizing the Labatto quadrature[18] was employed in the calculation of the powder average molar magnetic susceptibility[19]

$$\chi_{av} = \frac{1}{2}\int_0^{\pi} \chi_{\cos\theta} \sin\theta \, d\theta \qquad (3)$$

The advantage of this method over the more familiar Gaussian quadrature is the ability to evaluate the function at the limits of the integral, allowing for the calculation of the parallel and perpendicular components of the magnetic susceptibility.

The above formalism assumes only $S = {}^1/_2$ states on each dimer interact and thus best describes the low-temperature data since the $S \geq {}^3/_2$ states on each dimer are not populated. Therefore, the data in the temperature range 2–40 K (Figure 2) were fit with these formulae, and the resulting best-fit curve is shown in Figure 5. The theoretical curve through the experimental data points was obtained using the parameters $J'_x = +39.6$, $J'_y = +39.3$, and $J'_z = +37.6$ cm^{-1}, while the g value was not varied and held constant at 2.0. The anisotropic exchange parameters may be recast into the more familiar isotropic exchange parameter, J', and zero-field splitting parameters, D' and E', using the following relations

$$J' = {}^1/_3(J'_x + J'_y + J'_z) \qquad (4)$$

$$D' = -{}^1/_2(2J'_z - J'_x - J'_y) \qquad (5)$$

$$E' = -{}^1/_2(J'_x - J'_y) \qquad (6)$$

The effective exchange coupling between the two $S_a = S_b = {}^1/_2$ centers is found to be ferromagnetic with a singlet–triplet splitting ($2J'$) of +77.7 cm^{-1}. The ground-state triplet is zero-field split with $D' = +1.8$ and $E' = -0.15$ cm^{-1}.

In order to confirm the sign and magnitude of the ground-state zero-field splitting, the parameters obtained from the temperature dependent susceptibility fit were used to model the isothermal magnetization data. Since these data were acquired at temperatures between 2 and 10 K, they are particularly sensitive to the energy level splitting of the triplet ground state. The agreement between theory and experiment is excellent, as evident in Figure 6, and provides solid evidence for the $\langle 1,0|$ component of the triplet lying lowest in energy in zero magnetic field (i.e., $D' > 0$).

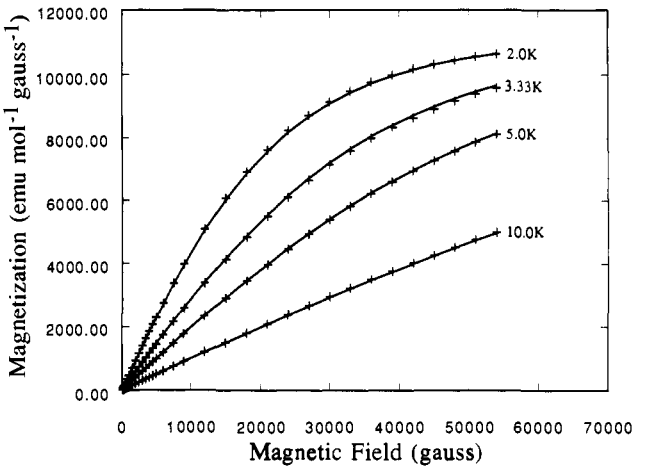

Figure 6. Isothermal magnetization vs applied magnetic field. Curves drawn through the data were generated using the fit parameters from Figure 5.

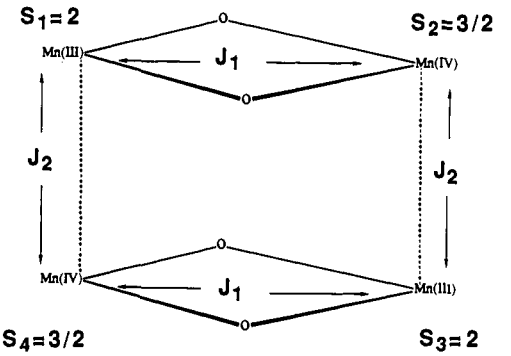

Figure 7. A complete representation of the interactions within the tetramer. The individual Mn centers are labeled by their spins, S_i, and the exchange constants, J_1 and J_2, which describe exchange interactions mediated through the oxo ligands and the alkoxide oxygens, respectively.

There exists an alternative description of the low-temperature (<15 K) effective magnetic moment behavior in cases where the individual tetrameric clusters are no longer magnetically isolated from one another. The effects of these intercluster interactions may be accounted for by use of a molecular mean field approximation.[20] Attempts directed toward modeling the low-temperature region with mean field theory resulted in poorer fits to the data than that obtained from the effective model incorporating anisotropic exchange (i.e., ZFS). Although we cannot entirely dismiss the presence of intercluster interactions on the basis of a poorer fit to the data, our results suggest it plays a less significant role than zero-field splitting in causing the drop in effective magnetic moment at lower temperatures. Furthermore, the singlet–triplet splitting determined from our calculations using two separate models appropriate for use in two different temperature regions are in excellent agreement, vide infra, while the molecular mean field approximation results in model dependent singlet–triplet splittings. The observed $g_{eff} \sim 6$ parallel polarization EPR resonance[12] coupled with the magnitude of the axial zero-field splitting parameter ($D' > h\nu$) are consistent with an assignment of the EPR transitions as originating from rhombically split $|T_x\rangle = -(1/\sqrt{2})[|+1\rangle - |-1\rangle]$ and $|T_y\rangle = (i/\sqrt{2})[|+1\rangle + |-1\rangle]$ levels of the ground-state triplet separated by $2E = 0.30$ cm^{-1}.

(17) Vermaas, A.; Groeneveld, W. L. *Chem. Phys. Lett.* **1974**, *27*, 583–585.
(18) Scarborough, J. P. *Numerical Mathematical Analysis*; Oxford University Press: New York, 1971; p 159.
(19) Marathe, V. R.; Mitra, S. *Chem. Phys. Lett.* **1974**, *27*, 103–106.
(20) (a) Moriya, T. *Phys. Rev.* **1960**, *117*, 635. (b) Carlin, R. L.; O'Connor, C. J.; Bhatia, S. N. *J. Am. Chem. Soc.* **1976**, *98*, 3523–3525.

Origin of the Effective Exchange Parameters. A complete representation of the exchange interactions within the tetramer is shown schematically in Figure 7, where the individual manganese centers are labeled by their spins, S_i, and the exchange constants, J_1 and J_2, describe exchange interactions mediated through the oxo ligands and the alkoxide oxygens, respectively. The effective exchange Hamiltonian (eq 1) operating on a fictitious basis describes the degeneracy and energy level splitting of the spin states but does not directly yield information concerning the sign or magnitude of the Mn(III)–alkoxide–Mn(IV) exchange interaction (J_2). In order to determine the relationship between J' and J_2, the $\langle S_a = {}^1/_2\ m_{sa} = \pm{}^1/_2, S_b = {}^1/_2\ m_{sb} = \pm{}^1/_2|$ basis must be related to the full four spin $\langle S_1\ m_{s1}, S_2\ m_{s2}, S_3\ m_{s3}, S_4\ m_{s4}|$ tetramer basis where $S_1 = S_3 = 2$ and $S_2 = S_4 = {}^3/_2$. Only certain $\langle S_1\ m_{s1}, S_2\ m_{s2}, S_3\ m_{s3}, S_4\ m_{s4}|$ functions contribute since the condition $|m_{s1} + m_{s2}| = {}^1/_2$ and $|m_{s3} + m_{s4}| = {}^1/_2$ must be met (i.e., $S_a = S_b = {}^1/_2$). The expression relating the two bases is given below

$$\langle S_a m_{sa}, S_b m_{sb}| = \sum_{m_{s1}+m_{s2}=-1/2}^{+1/2} \sum_{m_{s3}+m_{s4}=-1/2}^{+1/2} \delta_{m_{s1}+m_{s2}+m_{s3}+m_{s4}, m_{sa}+m_{sb}} \langle S_a m_{sa}|\langle S_1 m_{s1}, S_2 m_{s2}\rangle \langle S_b m_{sb}|S_3 m_{s3}, S_4 m_{s4}\rangle \langle S_1 m_{s1}, S_2 m_{s2}, S_3 m_{s3}, S_4 m_{s4}| \quad (7)$$

where δ is the Kronecker delta and each $m_{si} + m_{sj} = \pm{}^1/_2$ sum contains four terms. As a result, each $\langle S_a = {}^1/_2\ m_{sa} = \pm{}^1/_2, S_b = {}^1/_2\ m_{sb} = \pm{}^1/_2|$ basis function is comprised of a sum of 16 full tetramer basis functions ($\langle S_1\ m_{s1}, S_2\ m_{s2}, S_3\ m_{s3}, S_4\ m_{s4}|$), each of which is weighted by a product of two Clebsch–Gordon coefficients. Operating with the exchange Hamiltonian

$$\mathcal{H} = -2J_2(S_1 \cdot S_4 + S_2 \cdot S_3) \quad (8)$$

on the basis functions described on the right hand side of eq 7 and equating the value of the singlet–triplet splitting to that obtained from the effective exchange Hamiltonian (eq 1) gives

$$J' = -4J_2 \quad (9)$$

Equation 9 relates the exchange constant associated with an effective interaction between two $S = {}^1/_2$ dimer spins (J') to that between the manganese pairs bridged by the alkoxide oxygen (J_2). Using this formula, the Mn(III)–alkoxide–Mn(IV) exchange interaction is found to be -9.7 cm^{-1}. This is in excellent agreement with the value of -10 cm^{-1} for the exchange constant in the alkoxide bridged dimer complex $[Mn^{III}Mn^{IV}$[2-OH-3,5-Cl_2-(SALPN)]$_2$(THF)]ClO_4.[15] Therefore, an effective *ferromagnetic* J' corresponds to an actual *antiferromagnetic* interaction between alkoxide bridged sites within the tetramer.

At this point, we relax the constraint that only the $S = {}^1/_2$ states of the dimers are thermally populated in order to obtain information concerning the high spin states, determine the magnitude of the intradimer (Mn(III)–(μ-O)$_2$–Mn(IV)) exchange interaction, and to assess the accuracy of the effective model. We begin by utilizing the $S_1S_2(S_a),S_3S_4(S_b)$SM coupling scheme and construct *all* of the spin functions that comprise the full tetramer basis within this representation. S_a and S_b are intermediate coupled vectors, formed by coupling spins S_1 and S_2 and S_3 with S_4, respectively (Figure 7). The resultant vectors assume the values $S_{a,(b)} = S_{1,(3)} + S_{2,(4)}, \ldots|S_{1,(3)} - S_{2,(4)}|$. The total spin, S, is then formed by coupling S_a and S_b yielding values $S = S_a + S_b, \ldots|S_a - S_b|$. Griffith[21] has used the irreducible tensor method to derive closed-form expressions for calculating the matrix elements of the Hamiltonian in eq 10

$$\mathcal{H}_{ex} = \sum_{i=1}^{3} \sum_{j=i+1}^{4} -2J_{ij}(S_i \cdot S_j) \quad (10)$$

which extends eq 8 to include the intradimer exchange interactions (J_1) mediated by the oxo bridges. The individual J_{ij} describe the various exchange interactions between the S_i in the cluster. The full symmetry of the dimer-of-dimers exchange problem is realized when $J_{12} = J_{34} = J_1$, $J_{23} = J_{14} = J_2$, and the additional $J_{ij} = 0$. Under these constraints, the exchange Hamiltonian in eq 10 is not diagonal in the $S_1S_2(S_a),S_3S_4(S_b)$SM basis, containing off-diagonal terms in J_2 which mix states $|S_a,S_b,S\rangle$ with states $|S_a,S_b\pm1,S\rangle$, $|S_a\pm1,S_b,S\rangle$, and $|S_a\pm1,S_b\pm1,S\rangle$ within the same total spin manifold (S).[22]

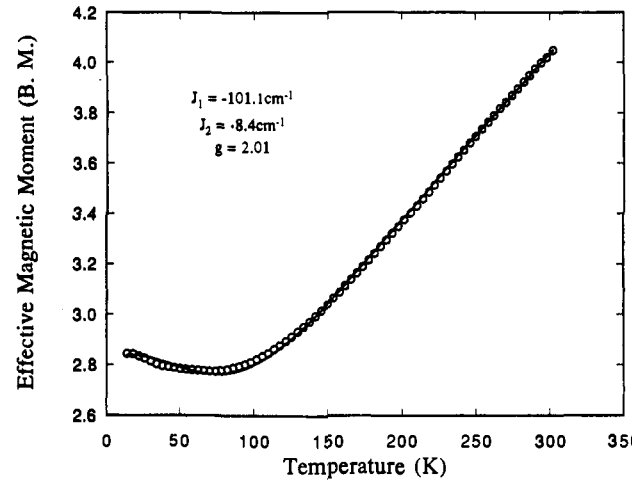

Figure 8. Fit of the effective magnetic moment (10–300 K) using the full tetramer basis described by the $S_1S_2(S_a),S_3S_4(S_b),SM_s$ coupling scheme.

The magnetic susceptibility data between 10 and 300 K were fit to the field independent Van-Vleck expression

$$\chi_{vv} = \frac{N\sum_n \frac{(E_n^{(1)})^2}{kT} \exp\left(\frac{-E_n^{(0)}}{kT}\right)}{\sum_n W_n \exp\left(\frac{-E_n^{(0)}}{kT}\right)} \quad (11)$$

where the $E_n^{(0)}$ are the exchange energies obtained from diagonalization of the individual total spin matrices, the $E_n^{(1)}$ are the first-order Zeeman coefficients, and the W_n are the associated state degeneracies. Although this susceptibility expression has the advantage of including all of the tetramer spin states, it does not include zero-field splitting and is not valid in the low-temperature region due to saturation effects (i.e., the model is linear in applied field). The best fit to the data for temperatures above 10 K is obtained with the parameters $J_1 = -101.1$ cm^{-1}, $J_2 = -8.4$ cm^{-1}, and $g = 2.01$, and is shown in Figure 8.

Excellent agreement is obtained between the interdimer exchange constant (J_2) derived from the full spin coupled basis approach and that obtained from the effective exchange model (-8.4 as compared to -9.7 cm^{-1}). The J_1 value is somewhat lower than that observed in Mn(III/IV) di-μ-oxo dimers.[9] A schematic diagram showing the lowest energy levels deriving from the total spin states $S = 0$, 1, 2, and 3 is presented in Figure 9. On the left is given the diagonal J_2 interactions that connect the intermediate spin states S_a and S_b, and the state energies which result are given to the right. The ground state triplet, derived from $S_a = {}^1/_2$ and $S_b = {}^1/_2$, is found to be separated from the first excited singlet, triplet, and quintet spin manifolds by $8J_2$ ($\sim$68 cm^{-1}), $3J_1 + 3J_2$ ($\sim$329 cm^{-1}), and $3J_1 + 1.4J_2$ ($\sim$315 cm^{-1}), respectively. The effect of the off-diagonal matrix elements is to modify somewhat the energies on the right of Figure 9. The presence of the off-diagonal elements connecting the degenerate $|S_a = {}^1/_2, S_b = {}^3/_2, S = 1,2\rangle$ and $|S_a = {}^3/_2, S_b = {}^1/_2, S = 1,2\rangle$ states results in a *g-u* resonance splitting that removes their degeneracy. Although in the low-temperature limit the dimer $S = {}^1/_2$ spins are effectively thermally isolated, the low-lying triplet and singlet are not pure $|{}^1/_2,{}^1/_2,1\rangle$ and $|{}^1/_2,{}^1/_2,0\rangle$ states due to mixing in of excited states. The $|{}^1/_2,{}^3/_2,1\rangle$, $|{}^3/_2,{}^1/_2,1\rangle$, and $|{}^3/_2,{}^3/_2,1\rangle$ excited states and the $|{}^3/_2,{}^3/_2,0\rangle$ excited state mix with the ground-state triplet and singlet, respectively. The singlet–triplet splitting determined by this formalism is 76.9 cm^{-1}. The effective coupling model described in Figure 4 gave a value of 77.7 cm^{-1} for the singlet–triplet splitting and, as such, gives an excellent description of the lowest

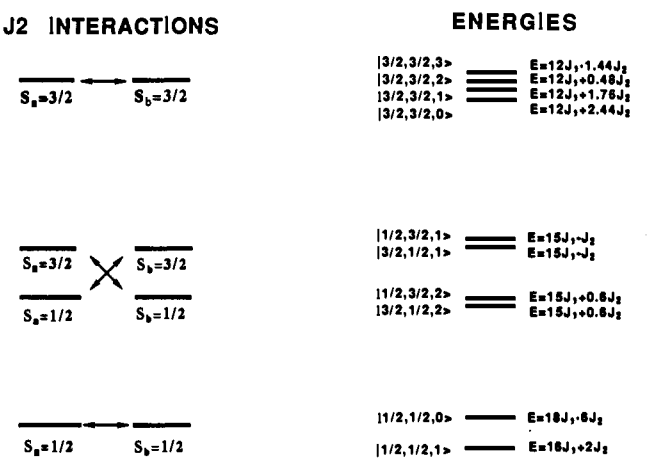

Figure 9. (Left) diagonal J_2 interactions connecting intermediate spin states, S_a and S_b, which arise from the dominant J_1 interaction and (right) an energy level diagram showing only the lowest levels deriving from the total spin states S = 0–3.

components of the ground state. However, the mixing of excited-state wave functions into the $|^1/_2,^1/_2,1\rangle$ state provides a mechanism for the zero-field splitting of the ground-state triplet, as is presented in the following section.

Origin of the Ground-State Zero-Field Splitting. The zero-field splitting of the $|^1/_2,^1/_2,1\rangle$ triplet ground state is found to be +1.8 cm^{-1}. There are three potential contributions to this zero-field splitting, namely, dipolar coupling, Mn(III) and Mn(IV) single-ion anisotropy, and pseudodipolar coupling. In this section we attempt to evaluate these various mechanisms.

A direct contribution to the zero-field splitting of the $|^1/_2,^1/_2,1\rangle$ triplet ground state arises from the spin dipolar coupling between the $S_a = {}^1/_2$ and $S_b = {}^1/_2$ intermediate states that represent each dimer core. An estimate of the dipolar contribution to D' can be readily determined from the distance between the alkoxide bridged dimers according to eq 12[23]

$$D_d = \frac{-3g^2\beta^2}{2r^3} \tag{12}$$

where the $^3/_2$ is a coefficient that depends on S_a, S_b, and S, and relates to the S = 1 triplet ground state. The distance between these cores (r) is 3.97 Å,[12] resulting in a dipolar interaction of −0.042 cm^{-1} (assuming g = 2). This value is of both the wrong sign and order of magnitude when compared to the experimental D'. Therefore, spin dipolar coupling between the two $S = {}^1/_2$ dimer cores does not determine the zero-field splitting of this system.

Each Mn center possesses a zero-field splitting which can contribute to the zero-field splitting of the S_a and S_b states associated with each dimer. For such a splitting to occur, the S_a and S_b states must have spin values greater than $^1/_2$, thus there exists no direct single ion contribution to the $|^1/_2,^1/_2,1\rangle$ state. This follows directly from vector coupling arguments. However, an indirect contribution to the ground-state zero-field splitting results from mixing excited spin triplets with S_a or S_b values greater than $^1/_2$ into the ground-state $|^1/_2,^1/_2,1\rangle$ wave function. This mixing makes single ion zero-field splitting, dipolar, and pseudodipolar contributions to the ground-state zero-field splitting. Referring to Figure 9 (right), off-diagonal matrix elements containing terms in J_2 mix the $|^1/_2,^3/_2,1\rangle$, $|^3/_2,^1/_2,1\rangle$, and $|^3/_2,^3/_2,1\rangle$ states with the ground-state triplet. The zero-field splitting of the ground-state triplet, $D_{|^1/_2,^1/_2,1\rangle}$, is given in eq 13

$$D_{|^1/_2,^1/_2,1\rangle} = E'_{|^1/_2,^1/_2,1,m_s=\pm1\rangle} - E'_{|^1/_2,^1/_2,1,m_s=0\rangle} \tag{13}$$

where $E'_{|^1/_2,^1/_2,1,m_s=\pm1\rangle}$ and $E'_{|^1/_2,^1/_2,1,m_s=0\rangle}$ are the perturbed energies of the $|m_s = \pm1\rangle$ and $|m_s = 0\rangle$ components of the triplet ground state. Expressions for these perturbed energies, which involve exchange mixing of these excited-state triplets into the ground state, may be derived from perturbation theory and are given in eqs 14 and 15.

$$E'_{|^1/_2,^1/_2,1,m_s=\pm1\rangle} = 2(36)J_2^2/[3J_1 + 3J_2 - (D_{|^1/_2,^3/_2,1\rangle}/3)] + 40J_2^2/[6J_1 + 0.24J_2 - (D_{|^3/_2,^3/_2,1\rangle}/3)] \tag{14}$$

$$E'_{|^1/_2,^1/_2,1,m_s=0\rangle} = 2(36)J_2^2/[3J_1 + 3J_2 + (2D_{|^1/_2,^3/_2,1\rangle}/3)] + 40J_2^2/[6J_1 + 0.24J_2 + (2D_{|^3/_2,^3/_2,1\rangle}/3)] \tag{15}$$

In these experiments, the numerators are the square of the matrix elements ($\langle S_a = {}^1/_2, S_b = {}^1/_2, S = 1|\mathcal{H}|S_a = {}^1/_2, S_b = {}^3/_2, S = 1\rangle = \langle S_a = {}^1/_2, S_b = {}^1/_2, S = 1|\mathcal{H}|S_a = {}^3/_2, S_b = {}^1/_2, S = 1\rangle = 6J_2$, and $\langle S_a = {}^1/_2, S_b = {}^1/_2, S = 1|S_a = {}^3/_2, S_b = {}^3/_2, S = 1\rangle = 2\sqrt{10}J_2$) that connect an excited-state triplet with the ground-state triplet. These matrix elements are the ones calculated from the closed-form expressions given by Griffith.[21] The denominators are the energy differences between the two states given in Figure 9 plus the zero-field splitting of each excited-state triplet.

Using the expressions derived by Scaringe et al.,[24] which extend the familiar Judd–Owen equations to include heterospin systems, the zero-field splittings of the $|^1/_2,^3/_2,1\rangle$, $|^3/_2,^1/_2,1\rangle$, and $|^3/_2,^3/_2,1\rangle$ states ($D_{|^1/_2,^3/_2,1\rangle}$ etc. in eqs 14 and 15) can be related to those of the uncoupled $\langle S_1\, m_{s1}, S_2\, m_{s2}, S_3\, m_{s3}, S_4\, m_{s4}|$ tetramer basis to give the single ion contributions to the excited-state zero-field splittings (eqs 16 and 17)

$$D_{|^1/_2,^3/_2,1\rangle} = D_{|^3/_2,^1/_2,1\rangle} = (-{}^9/_{10})D_{Mn(IV)} + ({}^{18}/_5)(D_{doxo} - D_{pdoxo}) \tag{16}$$

$$D_{|^3/_2,^3/_2,1\rangle} = ({}^{36}/_{25})D_{Mn(IV)} - ({}^{144}/_{25})(D_{doxo} + D_{pdoxo}) \tag{17}$$

where D_{doxo} and D_{pdoxo} are the dipolar and pseudodipolar interactions within the di-μ-oxo core and $D_{Mn(IV)}$ is the single ion zero-field splitting of the Mn(IV) ions. It should be noted that Mn(III), which may possess a large single-ion zero-field splitting, does not contribute to the zero-field splitting of the $|^1/_2,^3/_2,1\rangle$, $|^3/_2,^1/_2,1\rangle$, and $|^3/_2,^3/_2,1\rangle$ excited state triplets. This is a result of the coupling coefficient for $D_{Mn(III)}$ in eqs 16 and 17 being equal to zero.[24] This is not a general result of the theory, as other excited states possess a Mn(III) single-ion contribution of their zero-field splitting. However, none of these states mix into the ground-state triplet wave function. The dipolar (D_{doxo}) contribution within the di-μ-oxo dimer may be estimated from eq 18

$$D_{doxo} = -g^2\beta^2/r^3 \tag{18}$$

(21) Griffith, J. S. *Mol. Phys.* **1972**, *24*, 833–842.

(22) In general, the exchange Hamiltonian in eq 10 is not diagonal. However, under the following conditions the Hamiltonian is diagonal and the energies may be easily calculated (ref 21): (a) all J_{ij} are equal, (b) $J_{13} = J_{23} = J_{14} = J_{15}$, and (c) $J_{12} = J_{23} = J_{13}$ and $J_{14} = J_{24} = J_{34}$. The presence of off-diagonal matrix elements may have a profound effect on the EPR spectrum of tetranuclear complexes by mixing certain excited states into the ground-state wave function (vide infra).

(23) Use of the point dipole approximation for estimating the dipolar contribution to the ground-state zero-field splitting is reasonable whenever the distance between the two ions is large in comparison with the average distance of the unpaired electrons from their respective nuclei. A relevant example of the use of this approximation concerns the $Mn_2Cl_9^{5-}$ dimer doped into $CsCdCl_3$. In this case, the two Mn ions are in the 2+ (d^5) oxidation state, and the pair is separated by 3.26 Å. The experimentally determined value for the dipolar component of the zero-field splitting was found to be −0.04 cm^{-1}. This compares with the calculated value of −0.05 cm^{-1} using the point dipolar approximation. The point dipolar approximation neglects covalency effects. In open shell systems, finite amounts of unpaired spin density may be delocalized onto the bridging ligands. However, this effect has been treated in detail for the $V_2F_7^{3-}$ ion in $KMgF_3$ ($r \sim 4$ Å) using Hartree–Fock wave functions and results in a small (11.5%) increase in dipolar energy. Additionally, Extended Hückel calculations on fluoro-bridged copper dimers resulted in no appreciable deviation from the point dipolar approximation. Based upon these results, the fact that the d orbitals of $[(Mn_2O_2)_2(tphpn)_2]^{4+}$ are contracted due to the high oxidation states of the Mn ions (+3,+4), and the long 3.97 Å distance between alkoxide bridged Mn(III) and Mn(IV) ions, we believe the point dipolar approximation is reasonable for estimating the dipolar energies of this system well within a factor of 2. (a) For the $Mn_2Cl_9^{5-}$ dimer, see: McPherson, G. L.; Chang, J. R. *Inorg. Chem.* **1976**, *15*, 1018–1022. (b) For the $V_2F_7^{3-}$ ion, see: Smith, S. R. P.; Owen, J. *J. Phys. C: Solid State Phys.* **1971**, *4*, 1399–408. (c) For the fluoro-bridged copper dimers, see: Bencini, A.; Gatteschi, D. In *EPR of Exchange Coupled Systems*; Springer-Verlag: Berlin, 1990; p 27.

(24) (a) Scaringe, R. P.; Hodgson, D. J.; Hatfield, W. E. *Mol. Phys.* **1978**, *35*, 701–713. (b) Bencini, A.; Gatteschi, D. In *EPR of Exchange Coupled Systems*; Springer-Verlag: Berlin, 1990; pp 48–57.

Scheme I

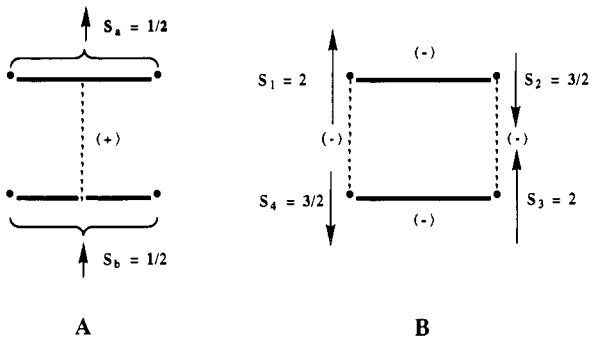

A B

and is found to be -0.09 cm^{-1} for $g = 2$, and a Mn(III)–Mn(IV) separation of 2.65 Å.[12] This expression differs from eq 12 since the latter describes the splitting of a triplet state, while eq 18 describes the interaction energy between two spin sites. The ground state of Mn(IV) in an octahedral field is an orbital singlet, and the energy differences between the ground and excited states are large when compared to the spin-orbit coupling which mixes orbital angular momentum into the ground-state wave function. This results in a small Mn(IV) zero-field splitting on the order of 0.1 cm^{-1}. Substituting -0.1 cm^{-1} for $D_{Mn(IV)}$ and D_{doxo} into eqs 16 and 17 and using the results in eqs 13, 14, and 15 gives $D_{|^1/_2,^1/_2,1\rangle} = 0.015$ cm^{-1}. Clearly, dipolar coupling within the di-μ-oxo core and single ion zero-field splitting have a very small effect on the zero-field splitting of the $|^1/_2,^1/_2,1\rangle$ ground state.

It is evident from eqs 13–17 that values of the pseudodipolar interaction within the di-μ-oxo core (D_{pdoxo}) on the order of a few wavenumbers would have a significant effect on the zero-field splitting of the tetramer ground-state triplet. There can also be a pseudodipolar contribution to the zero-field splitting of the triplet ground state deriving from interactions between the di-μ-oxo dimers mediated by the alkoxide oxygen of the tphpn ligand. In a manner analogous to that used to relate the fictitious (J') and actual (J_2) exchange parameters in eqs 7–9, an expression relating the zero-field splitting parameter (D') obtained from the effective exchange formalism to the actual pseudodipolar coupling (D_{pd}) between the manganese ions bridged by the alkoxide oxygens can be developed. Operating with the pseudodipolar interaction Hamiltonian (eq 19)

$$\mathcal{H} = D_{pd}(3S_{1z}\cdot S_{4z} + 33S_{2z}\cdot S_{3z} - 3S_1\cdot S_4 - 3S_2\cdot S_3) \quad (19)$$

on the four basis functions on the right hand side of eq 7 gives $+4D_{pd}$ (triplet, $|1,0\rangle$), $0D_{pd}$ (singlet, $|0,0\rangle$), $-2D_{pd}$ (triplet, $|1,+1\rangle$), and $-2D_{pd}$ (triplet, $|1,-1\rangle$). Therefore, the zero-field pseudodipolar splitting of the ground-state triplet is $6D_{pd}$, and by comparison with the effective zero-field splitting parameter in eq 5

$$D' = -6D_{pd} \quad (20)$$

From eq 20, an interdimer pseudodipolar interaction of only 0.3 cm^{-1} is required to reproduce the experimentally observed value of 1.8 cm^{-1} for D'. Both pseudodipolar interactions derive from single ion spin-orbit coupling to an excited state which undergoes an excited-state exchange coupling to an adjacent Mn center.[25]

Discussion

The analysis of the magnetic susceptibility and magnetization data for the dimer-of-dimers complex $[(Mn_2O_2)_2(tphpn)_2]^{4+}$ shows a ground-state triplet arises from an apparent ferromagnetic exchange coupling between two $S = ^1/_2$ dimers which in turn result from strong antiferromagnetic interactions within each $Mn_2(\mu\text{-}O)_2$ core. The apparent ferromagnetic coupling between dimers is, in fact (eq 9), found to originate from antiferromagnetic exchange coupling between alkoxide bridged Mn(III) and Mn(IV) ions located on adjacent $Mn_2(\mu\text{-}O)_2$ units. This result is most easily realized topologically as depicted in Scheme I. Scheme IA gives a pictorial representation of the effective exchange formalism. Here, the two strongly antiferromagnetically exchange coupled dimers (represented by the bold lines) each possess spin $S = ^1/_2$. The two spins, labeled S_a and S_b, are allowed to interact (represented by the dashed line) and the effective pairwise interaction (J') was experimentally determined to be ferromagnetic (+), resulting in a parallel alignment of the S_a and S_b spins. The origin of this effective ferromagnetic interaction results from antiferromagnetic (–) interactions between all four spins. This is depicted in Scheme IB. The crystal structure (Figure 1) shows individual Mn(III) ($S = 2$) and Mn(IV) ($S = ^3/_2$) spins are related by inversion symmetry; therefore, each $S = 2$ spin is antiferromagnetically coupled (–) to two $S = ^3/_2$ spins. Addition of the resultant spin vectors in Scheme IB yields $S_T = 1$, a triplet ground state, in agreement with the effective formalism. The result that this complex may be modeled in the low-temperature region as a simple dimer-of-dimers is significant, since it shows that the electronic structure description parallels the dimer-of-dimers geometric arrangement of the cluster.

The exchange coupling constants for Mn(III/IV) di-μ-oxo dimer complexes range from -118 to -159 cm^{-1}.[9,26] The exchange coupling within the $Mn^{III/IV}_2(\mu\text{-}O)_2$ cores of $[(Mn_2O_2)_2(tphpn)_2]^{4+}$ ($J_1 = -101$ cm^{-1}) is significantly reduced. This is particularly interesting in comparison to $[(Mn_2O_2)_2(tmdp)_2(H_2O)_2]^{4+}$,[27] which possesses a J value (-148 cm^{-1}) within the range of the Mn(III/IV) di-μ-oxo bridged dimers. This is also a dimer-of-dimers structure, but the two alkoxide oxygens of the tmdp ligand are bound axially only to the Mn(IV) ions with H_2O replacing the alkoxide on the Mn(III) sites. As a result, the interdimer superexchange pathway is eliminated. The magnetic orbital pathway in the $Mn_2(\mu\text{-}O)_2$ core likely involves $d_{xz,yz}$–Op_z–$d_{xz,yz}$ where the z-axis is oriented perpendicular to the core plane. It might be expected that structural perturbations at each Mn center which affect the orientation of the metal $d_{xz,yz}$ orbitals relative to the O2p orbitals are responsible for the reduction in J_1. However, there does not appear to be a single parameter magnetostructural correlation in Mn(III/IV) di-μ-oxo bridged dimers which relates the exchange mediated by the di-μ-oxo ligands to structural features such as the Mn–oxo and Mn–Mn distances, the Mn–oxo–Mn angle, or the nonplanarity of the $\{Mn_2O_2\}$ core.[9,12] Specifically, the structural features of $[(Mn_2O_2)_2(tphpn)_2]^{4+}$ are similar to those of $[(Mn_2O_2)_2(tmdp)_2(H_2O)_2]^{4+}$. The most prominent difference between these two dimer-of-dimers complexes involves the electronic difference between bridging and terminal alkoxides bound to Mn(IV) and the lack of an alkoxide on the Mn(III) ions in $[(Mn_2O_2)_2(tmdp)_2(H_2O)_2]^{4+}$. In fact, the electronic spectrum of $[(Mn_2O_2)_2(tphpn)_2]^{4+}$ differs from that observed in di-μ-oxo dimer complexes,[12b] reflecting an electronic perturbation of the di-μ-oxo core. The J_2 value of -8.4 cm^{-1} for $[(Mn_2O_2)_2(tphpn)_2]^{4+}$, which describes the interdimer exchange coupling mediated by the alkoxide oxygens, is antiferromagnetic, as would be expected, and is in excellent agreement with the exchange interaction ($J = -10$ cm^{-1}) recently obtained for the alkoxide bridged dimer $[Mn^{III}Mn^{IV}[2\text{-}OH\text{-}3,5\text{-}Cl_2\text{-}(SALPN)]_2\text{-}(THF)]ClO_4$.[15]

Although the relative magnitudes of the two different exchange interactions result in a dimer-of-dimers electronic structure description of the tetramer, the origin of the ground-state zero-field splitting is more complex. One might have expected the zero-field splitting to reflect the dipolar interaction between the $S = ^1/_2$ spins of the two dimer cores at an interdimer separation of 3.97 Å. However, the zero-field splitting of the $[(Mn_2O_2)_2(tphpn)_2]^{4+}$ ground-state triplet is considerably larger than that predicted based on the known structural properties of the tetramer.[12] Thus, structural insight cannot be obtained from the magnitude of the zero-field splitting when this term reflects either single ion zero-field splitting or pseudodipolar interactions. Since no Mn(III) or Mn(IV) zero-field splittings contribute to the $|^1/_2,^1/_2,1\rangle$ ground state, we have allowed for mixing of zero-field split excited-state triplets into the ground-state wave function via a perturbative

(25) (a) Bleaney, B.; Bowers, K. D. *Proc. R. Soc. London, A* **1952**, *214*, 451–465. (b) Owen, J.; Harris, E. A. In *Electron Paramagnetic Resonance*; Geschwind, S., Ed.; Plenum: New York, 1972; pp 427–492.

(26) Thorp, H. H.; Brudvig, G. W. *New. J. Chem.* **1991**, *15*, 479–490.

mechanism. The zero-field splitting of monomeric Mn(III) complexes can be quite large, on the order of 10 cm^{-1} [28] and would be expected to make a large contribution to the splitting of the excited triplets. However, from the vector coupling relationships, there is no Mn(III) single-ion anisotropy contribution to those excited states ($|^1/_2,^3/_2,1\rangle$, $|^3/_2,^1/_2,1\rangle$, and $|^3/_2,^3/_2,1\rangle$) connected to the ground-state triplet by an off-diagonal matrix element in J_2. The zero-field splitting of six-coordinate Mn(IV) complexes is typically small ($D \sim 0.1$ cm^{-1}),[29] rendering this contribution ineffective toward generating any appreciable splitting of the triplet. Therefore, the major contribution to the ground-state zero-field splitting appears to be pseudodipolar coupling. This involves excited-state exchange interactions mediated by the di-μ-oxo bridge (D_{pdoxo}) and/or the alkoxide oxygen bridging ligands (D_{pd}) which tether the two cores. According to the perturbation expressions in eqs 13–17, the D_{pdoxo} contribution would have to be quite large to solely account for the 1.8-cm^{-1} splitting of the ground-state triplet. As a result, we favor the alkoxide mediated pseudodipolar coupling (D_{pd}) as the dominant contribution to the zero-field splitting of the $|^1/_2,^1/_2,1\rangle$ ground state. The value of D_{pd} need only be 0.3 cm^{-1} to produce the experimentally observed 1.8-cm^{-1} splitting of the ground-state triplet. Note that while the ground state J_2 is relatively small, it is an excited state J which is responsible for the pseudodipolar interaction and this can be considerably larger.

The results of this study indicate that the $g_{eff} \sim 6$ parallel polarization EPR resonance observed for $[(Mn_2O_2)_2(tphpn)_2]^{4+}$ [12] derives from transitions within a zero-field split triplet ground state, as this is the only magnetic state populated at low temperatures. The S_1 state of the MnWOC displays a parallel polarization EPR signal that has been simulated using an $S = 1$ spin-Hamiltonian.[7] This spectral similarity supports the notion that the manganese aggregate in PSII, like $[(Mn_2O_2)_2(tphpn)_2]^{4+}$, possesses a triplet ground state. It must be emphasized that although the EPR spectral properties of the PSII MnWOC at S_1 are consistent with an $S = 1$ ground state, the EPR yields no direct information concerning the exchange coupling scheme or the spatial arrangement of the Mn ions within the aggregate. The important point here is that the dimer-of-dimers (two $[Mn^{III}Mn^{IV}] = S' = 1/2$ cores) can result in such a triplet ground state which derives from a weak antiferromagnetic exchange coupling between the dimers.

Upon advancement from S_1 to S_2, the manganese aggregate in PSII is oxidized by one electron, presumably to the Mn(III,IV,IV,IV) oxidation level. From EXAFS studies at S_1 and S_2, it has been determined that there is no appreciable structural rearrangement accompanying the removal of one electron from the aggregate.[5b,c] Assuming a dimer-of-dimers structure similar to that of $[(Mn_2O_2)_2(tphpn)_2]^{4+}$ for the manganese cluster at S_2, the aggregate would consist of a di-μ-oxo Mn(III,IV) dimer core tethered to a Mn(IV,IV) di-μ-oxo unit. All of the known Mn(IV,IV) di-μ-oxo bridged dimers are strongly antiferromagnetically exchange coupled with $S = 0$ ground states.[9,26] Therefore, the manganese cluster might be expected to possess a $|S_a,S_b,S\rangle = |^1/_2,0,^1/_2\rangle$ doublet ground state with EPR hyperfine contributions from only the Mn(III,IV) core. Such a ground state would have EPR spectral properties that are essentially identical to a Mn(III,IV) di-μ-oxo dimer, consisting of a 16 line signal centered at $g = 2$. This is inconsistent with the observed $g = 2$ multiline resonance for the MnWOC at S_2, which is considerably broader and consists of at least 19 ^{55}Mn hyperfine lines. Recent EPR simulation of the $g = 2$ multiline feature and the $g = 4$ multiline signal indicates that four isotropic hyperfine parameters are required to adequately model the data.[6,30] This apparent inconsistency may be reconciled to some extent if one recalls from eq 10 that the exchange Hamiltonian appropriate for a dimer-of-dimers geometry is not diagonal with respect to the interdimer exchange. As a result, off-diagonal terms proportional to the square of the interdimer exchange mix $|S_a,S_b,S\rangle$ states with $|S_a,S_b\pm1,S\rangle$, $|S_a\pm1,S_b,S\rangle$, and $|S_a\pm1,S_b\pm1,S\rangle$ states within the same total spin manifold (S). Therefore, the true doublet ground state would contain some $|^3/_2,0,^1/_2\rangle$ character mixed into the $|^1/_2,0,^1/_2\rangle$ levels, as well as some $|1/2,1,1/2\rangle$ and $|3/2,1,1/2\rangle$ character with hyperfine contributions from all four Mn ions. This would result in an EPR spectrum of the doublet ground state that would deviate from the 16 line spectrum observed in isolated Mn(III,IV) di-μ-oxo dimers. However, this mixing involves only J_2 and the $|^1/_2,1,^1/_2\rangle$ and $|^3/_2,1,^1/_2\rangle$ contributions to the ground-state wave function would be expected to be small. This could increase if oxidation of Mn results in a larger value for J_2 by inductively decreasing the pK_a of one of the associated interdimer bridging ligands (if, for example, the alkoxides in Figure 1 were hydroxo ligands in the WOC) leading to its deprotonation.

There are two additional caveats with respect to the dimer-of-dimers structure for the Mn aggregate at S_2. The first concerns the observation of a perturbed S_2 state $g = 4.1$ EPR resonance. This resonance has been interpreted as arising from a perturbed conformation of the cluster and is consistent with transitions originating from the middle Kramers doublet of a rhombic $S = {}^5/_2$ system ($D \sim h\nu$).[6,31,32] A dimer-of-dimers geometric arrangement, such as that observed for $[(Mn_2O_2)_2(tphpn)_2]^{4+}$, would not account for this perturbed conformation induced spin variability. At S_2, a dimer-of-dimers structure would possess a well isolated ground-state doublet that would remain as such in the limit of minor structural perturbations. However, the origin of the $g = 4.1$ EPR resonance may reflect a severely perturbed conformation of the Mn aggregate at S_2, as this signal is present only in samples which have been modified by chloride depletion, use of sucrose as a cryoprotectant, fluoride substitution, or certain low-temperature illumination conditions.[3,6,33a] The second point associated with the dimer-of-dimers arrangement concerns the observed increase of 9–17 μ_β^2 per PSII complex accompanying the $S_1 \rightarrow S_2$ transition.[33] Such a large increase in the magnetic susceptibility has been interpreted as arising from reduced exchange coupling within the cluster. The reduced coupling is necessary in order to overcome the decrease in magnetism that accompanies the removal of one electron from the cluster. In the dimer-of-dimers model, the exchange coupling within a di-μ-oxo core would have to decrease by approximately 80% to account for the observed increase in paramagnetism following a one-electron oxidation of the Mn cluster. A Mn(IV,IV) or Mn(III,IV) di-μ-oxo dimer with such a greatly reduced exchange coupling constant has yet to be observed experimentally. The observed increase in the square of the effective moment would require a structural change that results in the incorporation of additional interdimer exchange pathways within the cluster. This could result in considerable changes in the ground-state magnetic properties depending on the relative magnitudes and signs of the exchange coupling constants. Such a structural rearrangement would, however, have to be consistent with EXAFS data which require that the Mn atoms of the MnWOC have between 1 and 1.5 Mn contacts at approximately 2.7 Å.[5c] One such structure that has additional exchange pathways is the cubane structure. This configuration possesses μ_3-oxo rather than μ_2-oxo bridges. Magnetic susceptibility studies on model distorted cubane structures show that the exchange interaction mediated by the μ_3-oxo bridges between Mn(III) and Mn(IV) ions ranges from

(27) Suzuki, M.; Hayashi, Y.; Munezawa, K.; Suenaga, M.; Senda, H.; Uehara, A. *Chem. Lett.* **1991**, 1929–1932.

(28) (a) Kirk, M. L.; Lah, M. S.; Raptopoulou, C.; Kessissoglou, D. P.; Hatfield, W. E.; Pecoraro, V. L. *Inorg. Chem.* **1991**, *30*, 3900–3907. (b) Bonadies, J. A.; Kirk, M. L.; Lah, M. S.; Kessissoglou, D. P.; Hatfield, W. E.; Pecoraro, V. L. *Inorg. Chem.* **1989**, *28*, 2037–2044. (c) Kennedy, B. J.; Murray, K. S. *Inorg. Chem.* **1985**, *24*, 1552–1557.

(29) Abragam, A.; Bleaney, B. In *Electron Paramagnetic Resonance of Transition Ions*; Dover Publications, Inc.: New York, 1986; pp 430–434.

(30) Bonvoisin, J.; Blondin, G.; Girerd, J.-J.; Zimmermann, J.-L., private communication.

(31) Hansson, O.; Aasa, R.; Vanngard, T. *Biophys. J.* **1987**, *15*, 825–832.

(32) Vanngard, T.; Hansson, O.; Haddy, A. In *Manganese Redox Enzymes*; Pecoraro, V. L., Ed.; VCH Publishers: New York, 1992; pp 105–118.

(33) (a) Baumgarten, M.; Philo, J. S.; Dismukes, G. C. *Biochemistry* **1990**, *29*, 10814–10822. (b) Sivaraja, M.; Philo, J. S.; Lary, J.; Dismukes, G. C. *J. Am. Chem. Soc.* **1989**, *111*, 3221–3225.

-21 to -30 cm^{-1}.[34] The reduction in exchange coupling can be explained by the fact that there is a decrease in e^- density at the μ_3-oxo resulting from its bridging to an additional Lewis acid metal ion. The EXAFS data do not eliminate the possibility of a highly distorted cubane structure at S_2.[5c]

In summary, the EXAFS data on oriented PSII preparations suggest the possibility of a dimer-of-dimers structure for the PSII WOC.[3-5] On the basis of the Mn K-edge inflection point energy and the edge shape, a Mn(III,IV,III,IV) oxidation state at S_1 has been suggested, although a Mn(III,III,III,III) oxidation state cannot be ruled out.[5b,c] Additionally, this state has been shown to be EPR active exhibiting an integer spin signal consistent with an $S = 1$ ground state.[7] Thus, an analogous dimer-of-dimers model complex has been synthesized[12] in the Mn(III,IV,III,IV) oxidation state which exhibits a similar EPR resonance. We have shown that an electronic model which reflects this general structure and oxidation state provides insight into the origin of this triplet EPR signal. Each Mn(III,IV) dimer is strongly antiferromagnetically exchanged coupled with $S' = {}^1/_2$, and the two dimers are weakly exchange coupled resulting in a low-lying singlet and triplet state. For the observed case of weak interdimer antiferromagnetic exchange coupling, the triplet state has been shown to be the ground state. Within this electronic structure description of a dimer-of-dimers, oxidation by one electron would produce an $S = {}^1/_2$ ground state analogous to that of MnWOC at S_2. The EPR of the ground-state doublet would possess hyperfine contributions from all four Mn ions due to mixing of specific excited-state doublets into the ground-state wave function. However, in order to explain the increase in the square of the effective magnetic moment upon going from S_1 to S_2, a significant but EXAFS indiscernible structural change would be required.

Acknowledgment. This research was supported by the National Science Foundation Grant DMB-9019752 (E.I.S.) and NIH Grant GM38275 (W.H.A.). E.I.S. and M.L.K. wish to thank J. J. Girerd for transmitting informative spin topology comments. W.H.A. was the recipient of a Searle Scholars Award (1986-1989) and a Presidential Young Investigator Award from the NSF. M.L.K. acknowledges the NSF for a postdoctoral fellowship (CHE-9002628—1990).

(34) Hendrickson, D. N.; Christou, G.; Schmitt, E. A.; Libby, E.; Bashkin, J. S.; Wang, S.; Tsai, H.; Vincent, J. B.; Boyd, F. D. W.; Huffman, J. C.; Folting, K.; Li, Q.; Streib, W. E. *J. Am. Chem. Soc.* **1992**, *114*, 2455-2471.

Radical Cage Effects in Adocobinamide (Axial-Base-Off Coenzyme B_{12}): A Simple Method for Trapping [Ado·Co^{II}] Radical Pairs, a New β-H Elimination Product from the Radical Pair and Measurement of an Unprecedentedly Large Cage-Recombination Efficiency Factor, $F_c \geq 0.94$

Cheryl D. Garr and Richard G. Finke*

Contribution from the Department of Chemistry, University of Oregon, Eugene, Oregon 97403-1253. *Received May 8, 1992*

Abstract: A simple method is reported for trapping organometallic caged radical pairs in adocobinamide (axial-base-off coenzyme B_{12}) Co-C bond thermolysis using high, ca. 1 M, concentrations of the stable nitroxide free radical TEMPO (2,2,6,6-tetramethylpiperidinyl-1-oxy). The product studies as a function of [TEMPO] resolve a literature controversy by showing that β-H elimination is not concerted, but rather proceeds through an [Ado· ·Co^{II}] caged pair. The method permits the first measurement of the thermal fractional cage-efficiency factor (F_c) for adocobinamide, $0.94 \leq F_c \leq 1.0$. This result, one of the few precise F_c values for metal-carbon homolysis in an organometallic complex and a rare F_c value for a bioorganometallic cofactor, is unprecedentedly large in comparison to all literature bond homolysis F_c values in solvents of comparable viscosity. It thereby serves to confirm the literature's prediction of sizable (≥ 0.5) F_c values in large, massive organometallic radicals.

Introduction

The concept of solvent-caged radical pairs, known for over half a century since Frank and Rabinowitch's original 1934 paper,[1] has enjoyed a broad applicability in organic chemistry. In organometallic and inorganic chemistry, however, our 1988 overview of the literature[2] revealed that solvent-cage effects are relatively little studied and often overlooked,[3] especially in metal-ligand (M-L) bond homolyses (i.e., as opposed to M-L heterolyses[4]), save a few notable exceptions.[5] The powerful tool of direct observation of caged radical pairs by pico- or femtosecond

(1) (a) Franck, J.; Rabinowitch, E. *Trans. Faraday Soc.* **1934**, *30*, 120. (b) Rabinowitch, E.; Wood, W. C. *Trans. Faraday Soc.* **1936**, *32*, 1381. (c) Rabinowitch, E. *Trans. Faraday Soc.* **1937**, *33*, 1225.

(2) Koenig, T. W.; Hay, B. P.; Finke, R. G. *Polyhedron* **1988**, *7*, 1499. See refs 1-14 therein for a list of lead references in the radical-cage chemistry area.

(3) This is especially true of studies of M-L bond dissociation energies by solution kinetic measurements; see ref 2 for a more complete discussion and references on this point.

(4) The fast kinetic studies of the San Diego groups of D. Magde and T. Traylor should be consulted for cage studies of M-L heterolyses: (a) Traylor, T. G.; Magde, D.; Taube, D. J.; Jongeward, K. A.; Bandyopadhyay, D.; Luo, J.; Walda, K. N. *J. Am. Chem. Soc.* **1992**, *114*, 417. (b) Bandyopadhyay, D.; Walda, K. N.; Magde, D.; Traylor, T. G.; Sharma, V. S. *Biochem. Biophys. Res. Commun.* **1990**, *171*, 306. (c) Traylor, T. G.; Taube, D. J.; Jongeward, K. A.; Magde, D. *J. Am. Chem. Soc.* **1990**, *112*, 6875. (d) Chatfield, M. D.; Walda, K. N.; Magde, D. *J. Am. Chem. Soc.* **1990**, *112*, 4680. (e) Jongeward, K. A.; Magde, D.; Taube, D. J.; Traylor, T. G. *J. Biol. Chem.* **1988**, *263*, 6027. (f) Jongeward, K. A.; Magde, D.; Taube, D. J.; Marsters, J. C.; Traylor, T. G.; Sharma, V. S. *J. Am. Chem. Soc.* **1988**, *110*, 380. (g) Traylor, T. G.; Magde, D.; Taube, D. J.; Jongeward, K. A. *J. Am. Chem. Soc.* **1987**, *109*, 5864. (h) Jongeward, K. A.; Marsters, J. C.; Mitchell, M. J.; Magde, D.; Sharma, V. S. *Biochem. Biophys. Res. Commun.* **1986**, *140*, 962. (i) Campbell, B. F.; Magde, D.; Sharma, V. S. *J. Biol. Chem.* **1985**, *260*, 2752. (j) Campbell, B. F.; Magde, D.; Sharma, V. S. *J. Mol. Biol.* **1984**, *179*, 143.

0002-7863/92/1514-10440$03.00/0